Binding Kinetics of Engineered Mutants Provide Insight about the Pathway for Entering and Exiting the Intestinal Fatty Acid Binding Protein†

Gary V. Richieri, Pamela J. Low, Ronald T. Ogata, and Alan M. Kleinfeld*

Torrey Pines Institute for Molecular Studies, 3550 General Atomics Court, San Diego, California 92121

Received November 12, 1998; Revised Manuscript Received March 1, 1999

ABSTRACT: To better understand the mechanism by which fatty acids bind to and dissociate from the binding cavities of fatty acid binding proteins (FABPs), we constructed 31 single amino acid mutants of the intestinal FABP (I-FABP) and determined the rate constants for binding and dissociation, primarily for long-chain fatty acids (FA). FA dissociation from these proteins was measured both by the ADIFAB method and by the change in tryptophan fluorescence of the FABPs. Rate constants for binding (k_{on}) were calculated from the rate constants for dissociation (k_{off}) and the equilibrium binding affinities. Amino acid substitutions were made at locations within the binding cavity, in the region of the gap between the βD- and βE-strands, and within the "portal" region of the protein. The k_{off} values for the mutant proteins ranged from about 20-fold slower to 4-fold faster than the wild-type (WT) protein. Values for k_{on} were as much as 20-fold slower than the WT protein, but in no case was k_{on} significantly faster than the WT. Mutants with slower and faster k_{off} values were generally those involving sites within the binding cavity and, relative to the WT protein, revealed higher and lower affinities, respectively. Reduced rates of binding were generally, but not exclusively, associated with sites within the portal region. For example, for F68A which is located closer to the opposite end of the protein from the portal region, the k_{on} is more than 10-fold slower than WT. Even for these distal sites, however, the evidence is consistent with reductions in k_{on} being due to alterations of the portal region. Binding affinities and rate constants measured as a function of ionic strength also suggest that the FA initially binds, through an electrostatic interaction, to Arg-56 on the surface of the protein, before inserting into the binding cavity. Thus, the results of this study are consistent with FA binding to I-FABP involving an initial interaction with Arg-56 followed by insertion of the FA, through the portal region, into the binding cavity and with a reversal of these steps for the dissociation reaction.

Fatty acid binding proteins (FABPs)[1] are approximately 15 kDa cytosolic proteins that are found in a wide variety of cells and likely play important roles in fatty acid (FA) metabolism (*1*−*4*). X-ray crystallography and NMR studies indicate that the dominant feature of the FABP structure is a "clam shell" formed by 10 orthogonal β-strands and a pair of α-helices which creates a FA binding site deep within the protein (*5*−*11*).

Although the details of how FABPs function in FA metabolism remain to be elucidated, it is generally thought that by binding and releasing FA, FABPs either transport FA between specific intracellular locations and/or provide a buffer for maintaining intracellular FFA levels (*4*, *12*). Because characteristic times of FA transport and metabolism are on the order of seconds (*13*), one would also expect binding to and dissociation from the FABPs to be at least this fast. Rate constants for FA binding and dissociation to a variety of FABPs are consistent with this expectation (*14*). In particular, rate constants for FA dissociation (k_{off}) from the rat intestinal FABP (rI-FABP) range from about 5 s^{-1} for oleate to 30 s^{-1} for linolenate, at 37 °C. Moreover, rate constants for binding (k_{on}) at 37 °C are on the order of 1.0×10^8 M^{-1} s^{-1} for the long-chain FA and, given the high intracellular concentrations of FABPs (*15*), imply times that are less than seconds for FA binding.

How the FA can enter and leave the I-FABP so rapidly is not immediately apparent from the apo and holo crystal images of this protein because no large entry way into the binding cavity is revealed by these images and because little or no conformational difference exists between the apo and holo states. However, because the binding cavity can be observed through an orifice formed by the region circumscribed by the α_{II} helix, and the neighboring turns between βC and βD and between βE and βF, Sacchettini et al. (*5*) identified this "portal region" of I-FABP as the probable site of entry for FA. As a static structure this orifice is too small to admit a FA, and it was expected that FA entering into and exiting from the cavity would be facilitated by the movement of a small number of side chains within the portal region without the need for large changes in conformation (*16*). This concept has been extended and refined by Cistola and his colleagues (*11*, *17*, *18*), who have determined the solution structures of the apo and palmitate complex of I-FABP using NMR and have monitored the binding kinetics

†This work was supported by Grant GM46931 from the National Institute of General Medical Sciences.

* To whom correspondence should be addressed.

[1] Abbreviations: ADIFAB, rat intestinal fatty acid binding protein labeled at Lys^{27} with acrylodan; FA, fatty acid; FABP, fatty acid binding protein; LA, linoleate (18:2); OA, oleate (18:1).

10.1021/bi982703n CCC: $18.00
Published on Web 04/14/1999

of a helixless mutant of I-FABP. These studies suggested that the FA enters through the portal region because, in the apo protein, this area exhibits a high degree of mobility.

Although the exit pathway might be distinct from the entry pathway, evidence suggests that exiting the protein also involves the portal region. In particular, Storch and colleagues have found that membranes containing anionic phospholipids stimulate the transfer of FA from FABPs to the lipid membranes (*19*). The mechanism by which this transfer is stimulated appears to involve positively charged amino acids within or near the portal region (*20*, *21*). Storch et al. have suggested that an interaction between the portal region and intracellular membranes may enhance the rate of FA dissociation from the FABP and thereby effectively target FA to specific membranes such as those of the mitochondria (*21*). Consistent with this mechanism, Cistola et al. (*18*) have found that k_{off} from the helixless mutant is more than 100-fold faster than WT, suggesting that the membrane−FABP interaction may promote FA transfer from the FABP to the membrane by altering the conformation of the portal's helix.

Our previous studies are also consistent with the portal region as the site of FA entry to the binding cavity (*14*). Thus, k_{on} for ADIFAB is about 10-fold lower than the underivatized I-FABP. This is consistent with a portal entryway because acrylodan is attached on helix II at location 27 and faces toward the βE−βF and βC−βD loops, and molecular simulations (not shown) of the apo I-FABP derivative are consistent with acrylodan wedged within the portal region. In addition, we found that the activation barriers for FA binding to WT adipocyte, heart, and the intestinal FABPs were similar, 7 ± 0.3 kcal/mol, and primarily enthalpic, suggesting that entry into the respective binding cavities involves a specific and similar conformational change. Given that similar portal regions have been identified in each of these proteins (*2*, *3*), these results suggested that entry to the binding cavity may involve similar alterations in the portal region of each protein. Liver FABP, for which the crystal structure suggests a greater degree of mobility in the portal region compared to other FABPs (*8*), also has a significantly smaller activation free energy for binding (6.3 ± 0.4 kcal/mol) and a significantly more favorable activation entropy than the other three FABPs (*22*). Finally, the activation enthalpy for binding to both ADIFAB and the WT proteins is dependent on the FA type, raising the possibility that entry into the cavity involves an initial binding step before the FA enters the cavity (*8*).

Structures of the cellular retinoid binding proteins are quite similar to the FABPs (*3*). Based upon higher crystallographic temperature factors for the βC−βD and βD−βE loops and molecular dynamics simulations, these proteins may undergo significant structural changes in the portal region as well as the gap between the βD and βE strands (*23*), raising the possibility that ligand entry/exit may involve the βD−βE gap.

Thus, although a variety of studies are consistent with the notion that the FA enters and exits the binding cavity through the portal region, current evidence cannot exclude alternative pathways. To further define the pathway of binding and dissociation, we have determined the rate constants for FA binding and dissociation from single amino acid mutants of I-FABP at locations that form the portal, βD−βE gap, and binding cavity regions. Results of these studies are consistent with FA first binding to Arg-56 on the surface, then entering the binding cavity through the portal region, and reversing these steps for dissociation.

METHODS

Materials. All measurements were done, as described previously (*24*−*26*), using the sodium salts of the FA purchased from Nu Chek Prep, Elysian, MN. All binding and kinetic measurements were done in a buffer consisting of 20 mM HEPES, 150 mM NaCl, 5 mM KCl, and 1 mM NaHPO4, at pH 7.4. The fluorescent FFA probe, ADIFAB, was prepared from acrylodan-derivatized recombinant rat intestinal fatty acid binding protein (rI-FABP) as described (*24*) and is available from Molecular Probes, Eugene, OR. All the I-FABP mutants were constructed, expressed, and purified as described previously (*24*−*26*). After isolation, the proteins were stored at 4 °C in buffer consisting of 50 mM Tris, 1 mM EDTA, 0.5 mM PMSF, and 0.05% sodium azide at pH 8.0. The I-FABP mutants were found to be stable; binding affinities for the I-FABP mutants were unchanged after several months of storage. In addition, we monitored the conformational stability of the WT and mutant proteins to denaturation by guanidine hydrochloride (Gdn-HCl) by measuring tryptophan fluorescence (λ_{ex} = 290 nm and λ_{em} = 340 nm) as described previously for 11 of the 34 I-FABP proteins used in the present study (*27*). Consistent with our previous results, for all 34 proteins no correlation was found between stability and binding affinity or between stability and rate constants (data not shown).

Determination of Rate Constants. Measurements of equilibrium binding of FA to FABP were done using ADIFAB fluorescence to monitor the binding of the FA to each FABP as described (*26*). Two independent stopped-flow fluorescence methods were used to detect the dissociation of the FA. In the first, we mixed FA/FABP complexes with ADIFAB and determined FA dissociation from the I-FABPs by monitoring the binding of FA to ADIFAB, as described previously (*14*). In the second method, we mixed FA/FABP complexes with rat liver FABP (L-FABP) and monitored the time course of tryptophan fluorescence. Because L-FABP has no tryptophan, the time course of tryptophan fluorescence could be used to determine k_{off} for the I-FABP proteins. k_{on} values were calculated as $k_{on} = k_{off}/K_d$, where K_d is the equilibrium dissociation constant.

Molecular Modeling Methods. Molecular simulations were done using the INSIGHT/DISCOVER 97 programs from Molecular Simulations Inc., San Diego, CA. Several choices exist for starting structures for these calculations including several apo and holo structures determined by X-ray crystallography and solution structures determined by NMR. In initial studies using NMR apo structures (PDB entry code AE10, for example), we observed that amino acid substitutions generated large changes, compared to the WT, in the energy-minimized structures. This was primarily due to an insufficient number of water molecules inserted into the binding cavity by the INSIGHT "soak" function. We therefore used for the simulations of the apo proteins, the 1.2 Å structure determined by X-ray crystallography (PDB entry code 1IFC) which includes 22 water molecules within the binding cavity (*28*). For the holo proteins, we used the crystallographic structure with bound palmitate (PDB entry

code 2IFB). For both the apo and holo structures, all crystallographic waters were used in the simulations.

To simulate amino acid substitutions, we applied the "residue replace" function of INSIGHT to the initial apo or holo structures and used the "soak" function to generate either a 5 or a 10 Å thick water shell around these proteins. This added approximately 823 or 1563 molecules of solvent water and, for mutants whose side chains were significantly smaller than the WT, up to 2 additional water molecules in cavity. The WT and "mutant" structures, together with the crystallographic and added water molecules, were subjected to energy minimization using DISCOVER These calculations were done with the CVFF force field using the following parameters: pH 7.0, no cutoff for the nonbonded interactions, and a convergence parameter of a maximum derivative of 0.1 kcal mol^{-1} $Å^{-1}$ for the conjugate gradient method. The energy-minimized structures were compared according to their backbone RMS differences and visual inspection of Connolly surfaces.

Molecular dynamics were simulated for between 200 ps and 1 ns for the WT and several mutants. The starting structures were the energy-minimized system of protein plus either the 5 or the 10 Å water shell, to which was added for the dynamics calculations an additional fixed 5 or 10 Å shell of water to prevent water from escaping from the inner (unconstrained) water shell. The dynamic calculations were done at 300 °C with the cell multipole summation method used for nonbonded interactions, a step size of 1 fs, and molecular coordinates saved every picosecond throughout the trajectory. These coordinates were used to trace the time courses of several atom to atom distances in the portal and gap regions and thereby gauge the effect of amino acid substitutions on the side chain and backbone dynamics in these regions. RMS changes relative to the starting structures were evaluated for each trajectory, and analyses of atom to atom distances were done using only the plateau portions of the trajectories for which RMS changes were ≤ 0.5 Å. Calculations were done using an SGI R10000-O2 work station and typically required about 10 h for optimization and 20 days for 1 ns dynamic runs.

RESULTS

Rates of Dissociation of Long-Chain FA from WT and Mutant I-FABP Proteins. Rate constants (k_{off}) for the dissociation of oleate and linoleate from I-FABP proteins were determined at 25 °C. The primary approach to determining k_{off} was to measure the time course for FA binding to ADIFAB following dissociation from I-FABP, as described previously for wild-type (WT) FABPs (*14*, *22*). These measurements demonstrate that single amino acid substitutions yield proteins for which k_{off} values range from about 100-fold slower to 4-fold faster than WT (Table 1, Figure 1). Proteins with significantly slower (>3-fold) k_{off} values were those (K27F, L72A, L102A, R106A, and Y117A) that also reveal significantly larger affinities than WT (Table 1). Significantly faster (>3-fold) k_{off} values were observed for I23A, D34A, F55G, R56A, and R126Q, all of which reveal smaller affinities.

Rate constants were also determined by monitoring the time course of tryptophan fluorescence intensity as oleate dissociates from the donor I-FABP protein and binds to L-FABP, which has no tryptophan (Table 2, Figure 2). The different proteins revealed changes in tryptophan intensity that differed considerably in magnitude and sign (Table 2). Reliable k_{off} values were obtained only for those proteins for which the intensity change was greater than about 10% in about 16 out of the 32 proteins investigated. In most cases, k_{off} values determined by tryptophan and ADIFAB were in reasonable agreement, differing by less than a factor of 2, although the tryptophan-determined values were larger. Moreover, in virtually all cases the changes in k_{off} determined by both methods were in agreement (Figures 1 and 2).

Rates of Binding of Long-Chain FA to WT and Mutant I-FABP Proteins. Rate constants for binding (k_{on}) were determined, primarily, by calculation as $k_{on} = k_{off}/K_d$ using the k_{off} and K_d values of Table 1. In addition, we measured k_{on} values in selected cases using the change in tryptophan fluorescence upon FA binding and for the acrylodan derivatives, WT (ADIFAB) and L72A mutant (ADIFAB2), by the

Table 1: Binding Affinities and Rate Constants for I-FABP Proteins[a]

	K_d (nM)		k_{off} (s^{-1})		k_{on} ($\times 10^{-7}$) (M^{-1} s^{-1})	
protein	OA[b]	LA[b]	OA	LA	OA	LA
WT	18	55	1.5	3.6	8.2	6.6
ADIFAB	233	767	2.4	6.9	1.0	0.9
ADIFAB2	32	85	0.58	1.1	1.8	1.3
N11A	28	87	2.3	5.9	8.1	6.8
Y14A	20	37	2	2.9	10	7.7
F17A	63	152	3.7	7.6	5.9	5
M18A	333	500	4	4.5	1.2	0.9
M21A	51	104	4.1	7.9	8	7.6
I23A	116	271	5.8	10	5	3.8
K27A	9	30	1.4	2.8	15	9.4
K27F	7	18	0.35	0.9	4.9	5.1
D34A	175	258	5.6	8	3.2	3.1
F47A	52	182	1.5	3.1	2.9	1.7
E51A	11	34	1.7	4.5	15	13
F55A	144	331	3.6	4.3	2.5	1.3
F55G	256	450	6.9	7.2	2.7	1.6
R56A	367	948	6.6	5.5	1.8	0.58
V60A	34	118	2.4	4	7	3.4
F62A	65	220	3	3.3	4.6	1.5
F68A	440	1230	4.4	3.2	1	0.26
Y70A	20	93	2.3	2.5	12	2.7
S71A	8	28	0.78	2	9.3	7.3
L72A	1	2	0.09	0.14	7	6.5
D74A	343	800	4.8	5.6	1.4	0.7
L78A	26	109	2.4	8.1	9.1	7.4
W82A	39	56	2.4	1.8	6.2	3.2
F93A	26	50	4.1	4.2	16	8.4
L102A	1	4	0.1	0.25	9	7.1
R106A	1	2	0.041	0.035	4.1	1.5
R106Q	71	127	4	5.4	5.6	4.3
Q115A	12	30	1.2	1.8	9.8	6
Y117A	2	7	0.21	0.7	8.9	11
R126A	243	347	3.4	5.9	1.4	1.7
R126Q	239	342	5.5	12	2.3	3.5

[a] Measurements of FA binding affinities and rate constants were done at 25 °C as described under Methods and previously (*14*, *26*). The K_d values, whose standard deviations ranged between 5 and 10%, were measured previously (*22*, *26*, *27*, *29*). k_{off} values were determined by averaging the results from the transfer of FA from FA/FABP complexes to ADIFAB for four different FA concentrations. The standard deviations from these multiple determinations were <30%. In several cases where the relative changes for oleate and linoleate were significantly different (see Figure 1), the sets of four measurements were repeated. Both sets of results for these cases (for example, F55G and R56A) yielded equivalent (differences < 30%) values. [b] FA are abbreviated OA (oleate) and LA (linoleate).

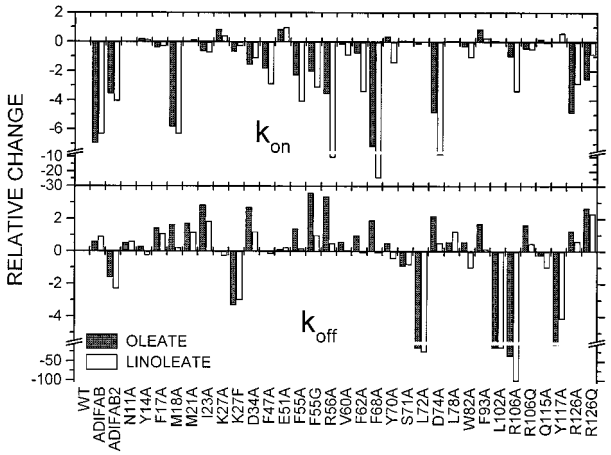

FIGURE 1: Relative change of k_{off} and k_{on} determined using ADIFAB. The values plotted here, for each of the 31 mutants and ADIFAB and ADIFAB2, are the quantities $k/k_{WT} - 1$ for $k > k_{WT}$ and $1 - k_{WT}/k$ for $k < k_{WT}$. The k_{off} values for the unlabeled proteins were measured using ADIFAB, and k_{on} values were calculated as k_{off}/K_d, as described under Methods. Values for the labeled proteins ADIFAB and ADIFAB2 were measured previously (14, 22). Results for k_{off} and k_{on} are shown in the upper and lower panels, respectively. Results are for measurements at 25 °C.

Table 2: k_{off} Values from the Change in Tryptophan Fluorescence[a]

protein	k_{off}[b] (s^{-1})	intensity change (%)[b]	protein	k_{off}[b] (s^{-1})	intensity change (%)[b]
WT	2.2	16	F62A	–	7
N11A	3.5	16	F68A	–	−3
Y14A	–	3	Y70A	–	−10
F17A	7.7	11	S71A	2	17
M18A	–	7	L72A	0.41	12
M21A	7.6	15	D74A	–	10
I23A	21	15	L78A	–	2
K27A	2.7	17	W82A	–	10
K27F	0.82	18	F93A	–	−7
D34A	–	8	L102A	0.35	11
F47A	2.9	15	R106A	0.21	−13
E51A	3	13	R106Q	8.7	−13
F55A	–	10	Q115A	–	2
F55G	–	3	Y117A	0.8	17
R56A	–	−2	R126A	–	8
V60A	5	17	R126Q	–	10

[a] Measurements of the time course of tryptophan fluorescence were done at 25 °C. Approximately 1 μM I-FABP protein complexed with oleate was stopped-flow-mixed with about 4 μM rat liver FABP. Tryptophan time courses were measured at four oleate concentrations between about 0.25 and 2 μM. The k_{off} values listed in this table are averages from the four time courses, and the standard deviations were ≤40%. Only cases in which the time course of the tryptophan intensity changed more than 10% yielded reliable k_{off} values. [b] The tryptophan fluorescence intensity changes are equal to $100 \times (I/I_0 - 1)$, where I_0 is the intensity in the absence of FA and I is the value at equilibrium in the presence of approximately saturating amounts of oleate.

change in R value. The calculated and directly measured k_{on} values are in good agreement (data not shown). The results reveal k_{on} values that are between about 20-fold slower to less than 2-fold faster than the WT I-FABP (Table 1, Figure 1). Proteins for which k_{on} is reduced significantly (>3-fold) primarily involve substitutions at sites that are part of the portal region, on the surface of the protein, or that have been derivatized with acrylodan.

Interactions with Medium-Chain FA and the Role of Phe-55. To investigate the possibility that F55 serves as a cap that limits the rate of dissociation from the binding cavity

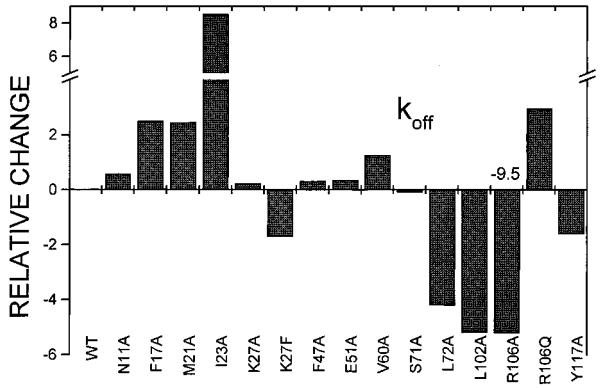

FIGURE 2: Relative change in k_{off} determined from the time course of tryptophan fluorescence. k_{off} values were determined as described under Methods, and the quantities plotted are $k/k_{WT} - 1$ for $k > k_{WT}$ and $1 - k_{WT}/k$ for $k < k_{WT}$, where k is k_{off}. Results are shown only for those proteins for which the change in tryptophan fluorescence was greater than 10%. Results are for measurements at 25 °C.

Table 3: Dependence of K_d and k_{off} on FA Chain Length for the WT and F55A Proteins[a]

FA	K_d(F55A)/K_d(WT)	k_{off}(F55A)/k_{off}(WT)
12:0	1.2	nd
14:0	2	0.8
16:0	5	2.4
18:0	9	10
18:1	9	2.4

[a] K_d values were measured at 37 °C and k_{off} at 25 °C for FA chain lengths between 12 and 18 carbons.

(*3*, *5*), we measured for the WT and F55A mutant binding affinities and dissociation rate constants for laurate (12:0) and myristate (14:0), in addition to the longer chain FA. Results of these measurements indicate that the reduction in affinity mediated by F55A decreases sharply with decreasing FA chain length, from a 9-fold reduction for 18:0 to a 20% reduction for 12:0 (Table 3). The reduction in affinity for F55A is in part due to an increase in k_{off} for the longer chain FA but not for 14:0 (Table 3). This suggests that interactions between the terminal end of the long-chain FA and Phe-55 stabilize the bound state rather than serving as a lid to prevent FA from exiting the binding cavity, consistent with the suggestion from the NMR structure (*17*).

Ionic Strength Dependence of Binding. Charged residues in the portal region or βD−βE gap might affect entry or exit from the binding cavity through electrostatic interactions (*5*). We therefore investigated binding and rate constants as a function of NaCl concentration for the WT protein and four mutants in which a charged residue was replaced by a neutral amino acid. The results of the binding affinity measurements reveal decreased binding affinities with increasing [NaCl] for all the proteins studied (Figure 3A). This decrease, as indicated by the slopes in this figure, is largest for WT, K27A, and D74A, about half this value for R106Q and R126A, and only about 25% of the WT dependence for R56A. This salt effect is probably due to a change in electrostatic interaction because any NaCl-mediated decrease in FA solubility should result in an increase in binding affinity. Thus, most of the solvent ionic strength dependence of binding appears to be due to Arg-56, a residue located on the surface of the βD strand, whose guanidinium group points

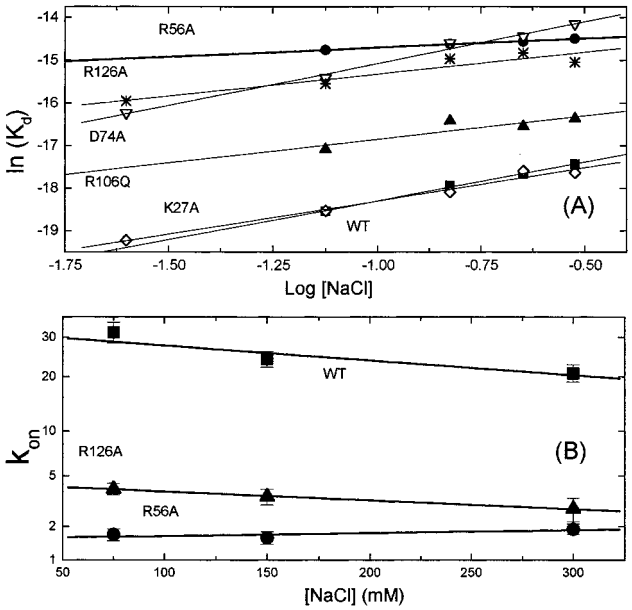

FIGURE 3: Dependence of binding affinities and k_{on} values on ionic strength. For the proteins indicated in the figures, K_d and k_{off} values were determined at 37 °C with increasing NaCl concentrations. These measurements were done using ADIFAB which was calibrated for different [NaCl] as described previously (30). The solid lines are linear fits to the data. K_d values are plotted in (A) and k_{on} values in (B).

toward the portal region (*28*). Moreover, although the rate of binding to the WT protein also decreases with [NaCl], k_{on} for R56A is essentially unchanged with increasing [NaCl] (Figure 3B). Both proteins, however, exhibit a similar rate of increase in k_{off} with [NaCl] (data not shown), suggesting that solvent shielding may be less effective for dissociation, in comparison to binding.

DISCUSSION

In this study we determined the rate constants for FA binding and dissociation from 31 single amino acid mutants of I-FABP. Amino acid substitutions were made at locations within the binding cavity, in the region of the gap between the D and E β-sheet strands, and within the "portal" region of the protein. Relative to the WT protein, k_{off} values for the mutant proteins ranged from about 20-fold slower to 4-fold faster. Values of k_{on} for the mutant proteins were as much as 10-fold slower than the WT, but in no case was k_{on} significantly faster than the WT. Mutants with slower and faster k_{off} values were generally those involving changes in the binding cavity and relative to the WT protein revealed higher and lower affinities, respectively. Amino acid substitutions that reduced k_{on} values relative to the WT were generally, but not exclusively, associated with sites in the portal region. Measurements as a function of ionic strength suggest that an electrostatic interaction between the FA and Arg-56 may be important for binding and dissociation. In what follows we discuss how these results help to describe the pathway by which FA enter and leave the binding cavity.

Pathway of FA Entry into the FABP Binding Cavity. Values for k_{on} are more than 10-fold slower than the diffusion-limited value and are sensitive to FABP type, indicating that specific amino acid side chains form the barrier for FA entry into the binding cavity (*14*, *22*). We therefore expect changes in k_{on} to reflect changes in the molecular interactions that form this barrier, and therefore by tracking values of k_{on} with side chain changes, it may be possible to map the pathway into the binding site. The acrylodan-derivatized WT and L72A and the following amino acid replacements, M18A, D34A, F47A, F55A, F55G, R56A, F68A, D74A, R126A, R126Q, yield proteins that significantly reduce k_{on} (>2-fold) relative to WT. Of these, ADIFAB, ADIFAB2, M18A, F55A, F55G, and D74A involve direct changes in the portal region (Figure 4A).

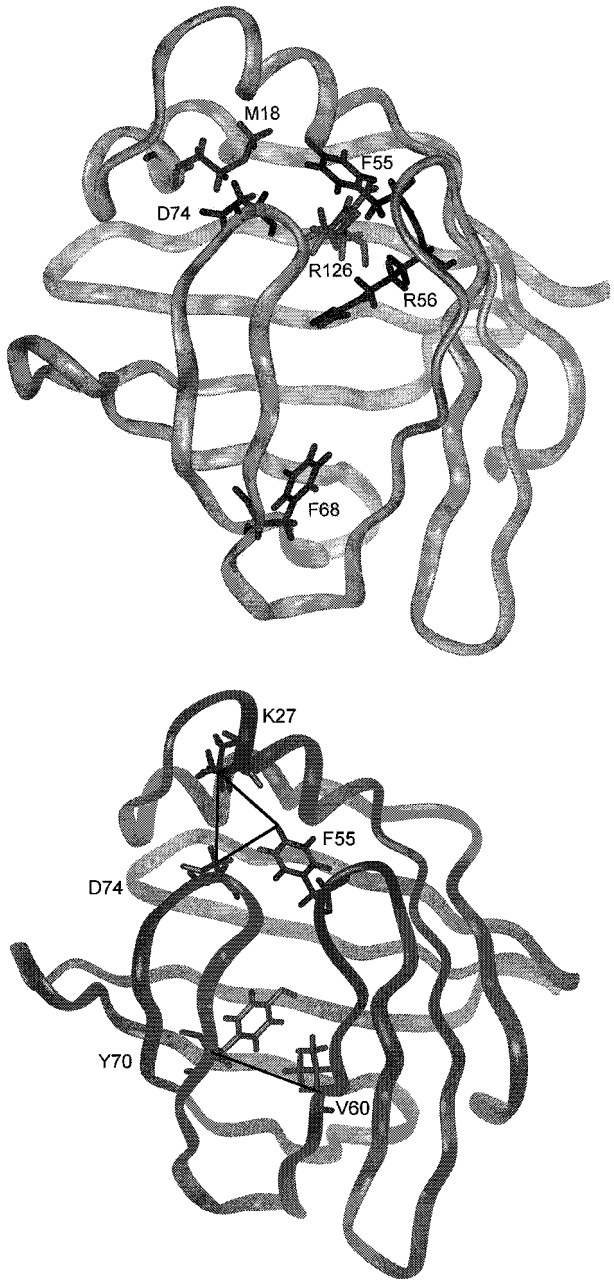

FIGURE 4: Images of I-FABP. These images were generated from the X-ray crystallographic coordinates (PDB 1IFC) of Scapin et al. (28). (A) Amino acid locations where Ala substitutions result in significantly smaller k_{on} relative to the WT protein. (B) Spacings used in the molecular dynamics simulations to define the portal and gap regions of the protein.

For ADIFAB and ADIFAB2, in which acrylodan is attached to position 27, molecular modeling predicts that acrylodan should insert into the orifice formed by the portal region (data not shown). Thus, the reduction in k_{on} that accompanies acrylodan derivatization of these proteins and

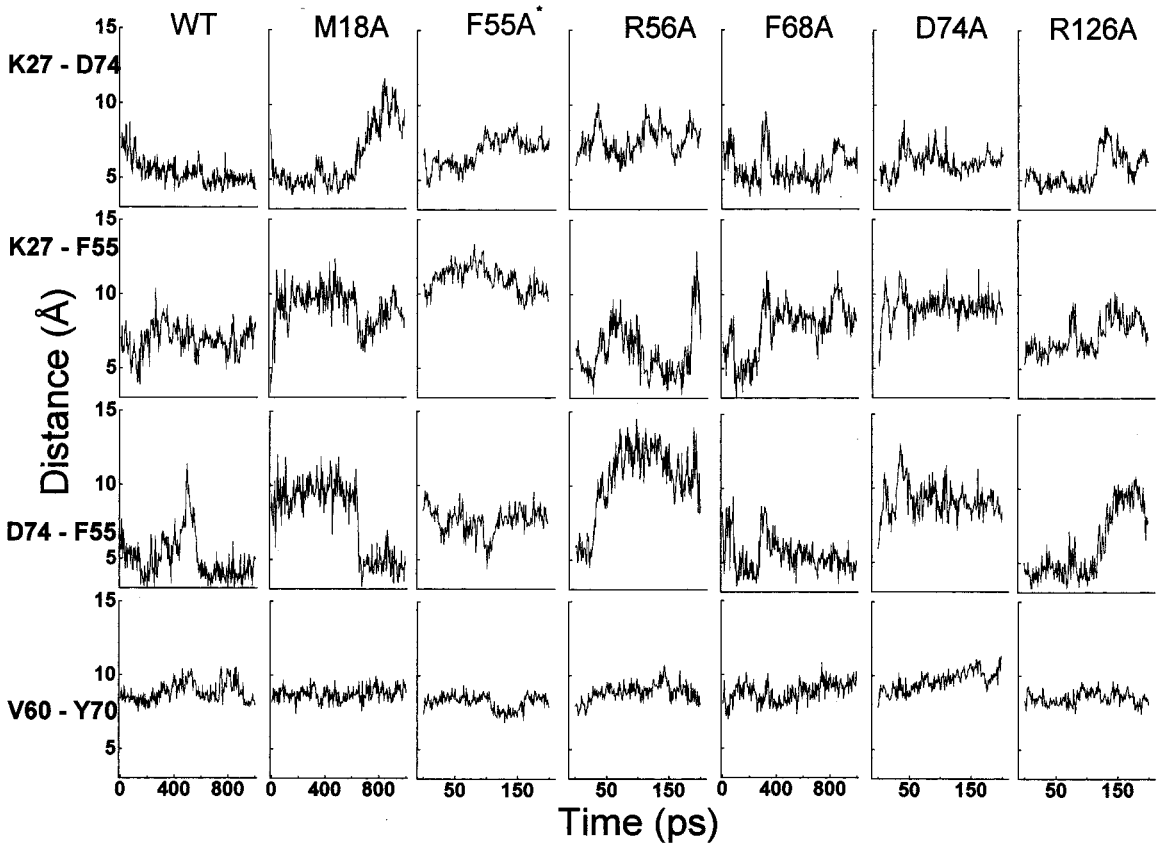

FIGURE 5: Results of molecular dynamics simulations of portal and gap regions of the apo I-FABP proteins. Calculations were done as described under Methods using the 1.2 Å structure of the WT protein determined by X-ray crystallography (28). Separations for F55A were calculated differently than for the other proteins, as explained in Table 4. Time courses were computed for atom−atom separations (see Table 4) in the portal region (K27−D74, K27−F55. and D74−F55) and the gap region (V60−Y70).

the occlusion of the portal's orifice predicted by molecular modeling are consistent with the portal region being the site of FA entry.

Apo structures of I-FABP determined by crystallography (*28*) and NMR (*17*) indicate that the Met-18, Phe-55, and Asp-74 side chains either insert into or form the portal region. Amino acid substitutions at these positions result in proteins (M18A, D74A, F55A, and F55G) for which k_{on} is substantially slower than for the WT (Figure 1). Although these results are consistent with the portal region as the entryway into the binding cavity, it is not clear, from simply viewing the apo structures, how the amino acid substitutions at these positions reduce k_{on}. For example, using molecular modeling to simulate Ala substitutions at these positions, followed by energy minimization, the resulting structure generally yields a larger portal opening than in the WT, rather than a smaller one as would be expected for smaller k_{on} values (data not shown). Furthermore, inspection of the crystallographic and solution structures of the apo protein does not predict specific side chain interactions involving these residues that might be expected to be altered by Ala substitutions in such a way as to reduce k_{on}.

Amino acid substitutions might, however, alter the dynamic characteristics of the portal region in such a way that critical distances between side chains would be reduced, on average, at physiologic temperatures. We investigated this possibility by carrying out molecular dynamics simulations for the WT and several mutants over times between 200 ps and 1 ns. Time courses were assessed for three atom−atom separations defining a triangle that roughly outlines the portal's orifice and a spacing roughly at the center of the βD−βE gap (Figure 4B). Although mutants that reduced k_{on} significantly might have yielded smaller separations by molecular dynamics simulations, results shown in Figure 5 and Table 4 indicate that neither the portal nor the gap dimensions are correlated significantly with k_{on} for these $\leq$1 ns simulations. These simulations do, however, reveal much greater mobility in the portal as compared to the gap region. Average fluctuation amplitudes for the portal spacings, as reflected for example in the standard deviations (Table 4), are greater than for the gap spacings. In addition, the portal spacings occasionally exhibit large (>5 Å) fluctuations above the average spacing, while in none of the WT or mutant trajectories (total time >8 ns) did we observe such fluctuations in the gap region that exceeded 2 Å. Although longer simulations will likely provide a more accurate assessment of the protein dynamics, these relatively short trajectories together with the experimental evidence support the notion that the slower k_{on} values of the mutants, relative to the WT protein, are more consistent with FA entry through the portal region than through the βD−βE gap.

In contrast to the direct connection to the portal region of the above amino acid substitutions, the effects of D34A, F47A, F68A, R126A, and R126Q are more difficult to rationalize in terms of the portal region. For example, the largest decrease in k_{on} observed in this study results from the Ala substitution for Phe at position 68, which is located at a site near the center−bottom half of the βD−βE gap (Figure 4A). This raises the possibility that the portal region might not represent a unique entryway, if it is assumed that

Table 4: Average Atom−Atom Distances (in Å) from Molecular Dynamics Simulations[a]

atoms[b]	wild type[d]	M18A[d]	F55A[d]	R56A[d]	F68A[d]	D74A[d]	R126A[d]
K27−D74	5.0 ± 0.6	6.7 ± 2.1	7.8 ± 0.6	7.8 ± 0.9	5.7 ± 0.9	6.3 ± 0.6	5.9 ± 1.2
K27−F55	7.0 ± 0.8	9.1 ± 1.2		6.1 ± 1.9	8.6 ± 1.0	9.2 ± 0.7	7.5 ± 1.1
	(10.3 ± 0.7)[c]		(10.9 ± 0.9)				
D74−F55	5.1 ± 1.7	7.7 ± 2.5		11.5 ± 1.4	5.3 ± 0.7	9.1 ± 0.8	6.8 ± 2.4
	(9.5 ± 1.8)		(8.4 ± 0.6)				
V60−Y70	9.0 ± 0.7	8.7 ± 0.5	8.0 ± 0.5	9.1 ± 0.6	9.0 ± 0.7	9.9 ± 0.6	8.5 ± 0.5

[a] Average atom−atom separations were calculated from the results of Figure 5. [b] Atom positions used were C_β of K27, C_β of D74, H_ζ of F55, C_β of A55, C_α of V60, and C_α of Y70. [c] For F55A, the C_β of A55 was used (instead of H_ζ of F55) for calculating separations, and we therefore also calculated the K27−F55(C_β) and D74−F55(C_β) separations for the WT protein for comparison with F55A. [d] Total simulation and plateau (when the RMS changes by ≤0.5 Å) times (in ps) were as follows: WT, 1000, 300; M18A, 1000, 100; F55A, 400, 150; R56A, 200, 75; F68A, 1000, 400; D74A, 200, 50; R126A, 200, 50.

the effect of the mutation is entirely local. However, as discussed previously, mutations of I-FABP at locations distal to the binding site can have substantial effects on binding affinities (*27*, *29*). For example, the D34A and R126A substitutions significantly alter binding thermodynamics, although neither of these positions is closer than 6.5 Å from the FA. We speculated that these substitutions disrupt the salt bridge/hydrogen bond network between D34 and R126, identified in the crystal structure (*28*), and this in turn alters the structure of the binding cavity. Another feature of the results is also consistent with nonlocal effects of amino acid substitutions for many of the mutant proteins. If the effect of a mutation were limited to changing the rate-limiting step for binding, then k_{on} and k_{off} should change symmetrically, but, as indicated in Figure 1, this is generally not the case. For example, k_{on} values for M18A and F68A are more than 7-fold slower than WT although k_{off} values actually increase slightly, and therefore for both proteins the binding affinity is significantly smaller than WT. These results imply that many of the mutations simultaneously alter the activation barrier and the interactions between the FA and protein within the binding cavity.

Based upon these results, significant structural alterations might be expected at sites distal to the amino acid substitutions. However, energy-minimized structures designed to simulate the D34A, F47A, F68A, and R126A mutations do not reveal significant structural changes in the portal or the βD−βE gap regions (data not shown), nor do these mutations significantly alter the protein dynamics of either the portal or the βD−βE gap (Figure 5, Table 4). In particular, neither energy-minimized structures nor protein dynamics reveal any significant F68A-mediated change of the βD−βE gap, and substitutions of residues that flank Phe-68 have virtually no effect on k_{on}. We assume that mutations that reduce k_{on} significantly probably mediate these changes by altering the dynamics of the portal region. These alterations may only be apparent, however, in longer time trajectories.

Although Arg-56, at the C-terminal end of the CD loop, may be part of the portal region, we consider it separately because this residue seems to embody most of the solvent-accessible electrostatic interaction, suggesting that the role of Arg-56 in FA binding may be distinct from other members of the portal region. Thus, Arg-56 may serve as the initial site of FA binding on the protein's surface, before the FA passes through the portal orifice. However, the crystal structure itself, which shows the guanidinium group of Arg-56 pointing inward to the cavity and within hydrogen-bonding distances of Tyr-70, Glu-51, and Ser-71, implies that Arg-56 might not be accessible to an interaction with the FA's carboxylate from the outside (*28*). This suggests that disruption of these hydrogen bonds would affect FA−FABP interactions, yet Y70A, E51A, and S71A have little effect on binding affinities and rates (Figure 1 and Table 1). Moreover, in contrast to the crystal structure result, the NMR structures show the guanidinium group of Arg-56 pointing outward from the surface, forming no salt bridges/hydrogen bonds with neighboring side chains (*17*), and therefore in a conformation amenable to an interaction of the FA carboxylate and Arg-56 at the surface. We suggest that the FA may bind, through the electrostatic interaction of the FA carboxylate and the guanidinium amides, to Arg-56 before entering the portal region. The relatively long-ranged electrostatic interaction may effectively increase the FA concentration near the portal region, and/or the FA-Arg-56 interaction may induce a change in orientation that moves the FA closer to the portal. Given the FA−molecular species dependence of k_{on} observed for the WT proteins (*14*, *22*), this initial step may also involve the interaction of the FA's hydrocarbon chain with other portions of the protein.

Pathway for FA Dissociation. FA dissociation from the binding cavity may occur through a reversal of the entry pathway or through an alternative pathway (*2*). Several studies indicate that the portal region may be involved in the dissociation process and raise the possibility that selective mutations in the portal region might affect the rate of FA dissociation (*18*, *20*, *21*). Consistent with this expectation, certain mutants in the present study (I23A, D34A, F55G, R56A, D74A, R126Q) increase k_{off} significantly (>3-fold) relative to WT. The effects of these mutants are probably not entirely local, because, as discussed above, the changes in k_{off} and k_{on} are asymmetric. Nevertheless, these results are consistent with a rate-limiting role for the portal region in dissociation because these mutations involve the portal region directly or, as discussed above and previously (*27*), severing the Asp-34−Arg-126 salt bridge seems to have widespread effects on the protein's structure. In no event do substitutions at sites involved in direct contact with the FA within the cavity result in increased k_{off} values. On the contrary, mutations of amino acids involved in the bound state either have no effect or reduce the k_{off} (L72A, L102A, R106A, Y117A), consistent with the exit site being rate-limiting for dissociation and separate from the binding cavity. Molecular dynamics calculations of the holo protein did not yield significant increases in the portal or gap regions for those mutants which resulted in increased k_{off} values, although, similar to the apo protein, fluctuations in the portal

region were significantly greater than in the gap region (results not shown). We speculate that this may reflect in part the difficulty of simulating the smaller changes in structure that are presumably associated with the smaller fractional changes in k_{off}, as compared to the larger changes observed for k_{on}.

Results for K27F and R56A provide more specific insights about the dissociation pathway. K27F was engineered because molecular simulations suggested that a phenyl group at position 27 might stack with Phe-55, at least for part of the trajectory. We speculated that this would cause a partial blockage of the portal's orifice and might reduce both k_{on} and k_{off}, if the effect of the mutation was localized to this site. As Figure 1 indicates, both k_{on} and k_{off} are reduced relative to the WT, making K27F one of the few mutants for which k_{on} and k_{off} are altered similarly, and is consistent with the portal region serving as both the entry and exit pathway. If exiting the binding cavity represents the time-reversed pathway for entry, the FA's carboxylate might bind to Arg-56 after leaving the portal's orifice, thereby slowing the rate of dissociation. Consistent with this notion, the R56A mutant reveals for oleate a more than 3-fold faster k_{off} than WT. Thus, involvement of Arg-56 in both the binding and dissociation steps suggests that the same, albeit time-reversed, pathways are used for FA entry into the exiting from the binding cavity.

Summary. In this study we have used the changes in binding and dissociation rate constants induced by single amino acid substitutions to help map the pathway for FA binding to and dissociation from I-FABP. The results suggest that upon desolvation from the bulk solvent, the FA forms a complex between its carboxylate and the guanidinium group of Arg-56. The FA then moves from this complex to the orifice of the portal region where it enters the binding cavity and adjusts its conformation to form the bound state observed by X-ray crystallography and NMR. We assume that binding to Arg-56 occurs before rather than after passage through the portal because increasing the ionic strength of the bulk solvent seems to shield Arg-56 but not residues within the cavity of portal region. Dissociation from the protein is consistent with a time-reversed trajectory of the binding process. Leaving the cavity involves severing interactions between the FA and amino acid side chains and water molecules in the bound configuration, followed, most likely, by the threading of the hydrocarbon chain back through the portal orifice. Although the efect of Arg-56 on dissociation is relatively modest, the increase in k_{off} upon Ala substitution is consistent with complex formation before FA dissociation from the protein. Arg or Lys at position 56 or an equivalent position is conserved in the FABP family, suggesting a similar role for the FA−Arg-56 interaction in all FABPs.

ACKNOWLEDGMENT

We thank Dr. Tom Woolf of the Johns Hopkins Medical School and Dr. Daan van Aalten of Cold Spring Harbor Laboratory for their insightful comments on the manuscript.

REFERENCES

1. Bass, N. M. (1988) *Int. Rev. Cytol. 111*, 143−184.
2. Sacchettini, J. C., and Gordon, J. I. (1993) *J. Biol. Chem. 268*, 18399−18402.
3. Banaszak, L., Winter, N., Xu, Z., Bernlohr, D. A., Cowan, S., and Jones, T. A. (1994) *Adv. Protein Chem. 45*, 89−151.
4. Glatz, J. F. C., and van der Vusse, G. J. (1996) *Prog. Lipid Res. 35*, 243−282.
5. Sacchettini, J. C., Gordon, J. I., and Banaszak, L. J. (1989) *J. Mol. Biol. 208*, 327−339.
6. Cowan, S. W., Newcomer, M. E., and Jones, T. A. (1993) *J. Mol. Biol. 230*, 1225−1246.
7. Young, A. C. M., Scapin, G., Kromminga, A., Patel, S. B., Veerkamp, J. H., and Sacchettini, J. C. (1994) *Structure 2*, 523−534.
8. Thompson, J., Winter, N., Terwey, D., Bratt, J., and Banaszak, L. (1997) *J. Biol. Chem. 272*, 7140−7150.
9. LaLonde, J. M., Bernlohr, D. A., and Banaszak, L. J. (1994) *Biochemistry 33*, 4885−4895.
10. Hodsdon, M. E., Toner, J. J., and Cistola, D. P. (1995) *J. Biomol. NMR 5*, 198−210.
11. Hodsdon, M. E., and Cistola, D. P. (1997) *Biochemistry 36*, 2278−2290.
12. Richieri, G. V., Ogata, R. T., and Kleinfeld, A. M. (1999) *Mol. Cell Biochem. 192*, 77−85.
13. Kleinfeld, A. M., Chu, P., and Romero, C. (1997) *Biochemistry 36*, 14146−14158.
14. Richieri, G. V., Ogata, R. T., and Kleinfeld, A. M. (1996) *J. Biol. Chem. 271*, 11291−11300.
15. Bass, N. M., Manning, J. A., Ockner, R. K., Gordon, J. I., Seerharam, S., and Albers, D. H. (1985) *J. Biol. Chem. 260*, 1432−1436.
16. Sacchettini, F. C., Scapin, G., Gopaul, D., and Gordon, J. I. (1992) *J. Biol. Chem. 267*, 23534−23545.
17. Hodsdon, M. E., and Cistola, D. P. (1997) *Biochemistry 36*, 1450−1460.
18. Cistola, D. P., Kim, K., Rogl, H., and Frieden, C. (1996) *Biochemistry 35*, 7559−7565.
19. Wootan, M. G., and Storch, J. (1994) *J. Biol. Chem. 269*, 10517−10523.
20. Herr, F. M., Matarese, V., Bernlohr, D. A., and Storch, J. (1995) *Biochemistry 34*, 11840−11845.
21. Herr, F. M., Aronson, J., and Storch, J. (1996) *Biochemistry 35*, 1296−1303.
22. Richieri, G. V., Ogata, R. T., and Kleinfeld, A. M. (1996) *J. Biol. Chem. 271*, 31068−31075.
23. van Aalten, D. M. F., Findlay, J. B. C., Amadei, A., and Berendsen, H. J. C. (1995) *Protein Eng. 8*, 1129−1135.
24. Richieri, G. V., Ogata, R. T., and Kleinfeld, A. M. (1992) *J. Biol. Chem. 267*, 23495−23501.
25. Richieri, G. V., Ogata, R. T., and Kleinfeld, A. M. (1994) *J. Biol. Chem. 269*, 23918−23930.
26. Richieri, G. V., Ogata, R. T., and Kleinfeld, A. M. (1995) *J. Biol. Chem. 270*, 15076−15084.
27. Richieri, G. V., Low, P. J., Ogata, R. T., and Kleinfeld, A. M. (1998) *J. Biol. Chem. 273*, 7397−7405.
28. Scapin, G., Gordon, J. I., and Sacchettini, J. C. (1992) *J. Biol. Chem. 267*, 4253−4269.
29. Richieri, G. V., Low, P. J., Ogata, R. T., and Kleinfeld, A. M. (1997) *J. Biol. Chem. 272*, 16737−16740.
30. Richieri, G. V., and Kleinfeld, A. M. (1995) *Anal. Biochem. 229*, 256−263.

BI982703N